ELSEVIER

Thermochimica Acta 357–358 (2000) 1–8

thermochimica acta

www.elsevier.com/locate/tca

Thermal characterization of an epoxy-based underfill material for flip chip packaging

Yi He*, Brian E. Moreira, Alan Overson, Stacy H. Nakamura, Christine Bider, John F. Briscoe

Assembly Test Materials Operation, CH5-232, Intel Corporation, 5000 W. Chandler Blvd., Chandler, AZ 85226-3699, USA

Received 13 September 1998; accepted 14 January 1999

Abstract

Epoxy-based underfill encapsulant materials are used in advanced microelectronic packaging to reduce thermal stresses on the solder joints and interconnections in integrated circuits. Therefore, their thermal properties directly affect package performance and reliability. In this study, the thermal properties of an epoxy-based underfill material developed for Intel's flip chip packaging were characterized using differential scanning calorimetry (DSC), thermogravimetric analysis (TGA), thermomechanical analysis (TMA), dynamic mechanical thermal analysis (DMTA) and DMA techniques. Experimental results showed that this epoxy can be cured rapidly with low cure weight loss. Near room temperature, the cured epoxy has a low coefficient of thermal expansion (CTE) and a moderate storage modulus, resulting in a low stress index. The glass transition temperature and thermomechanical properties as a function of epoxy curing conditions will be discussed.

Keywords: Epoxy-based underfill; Flip chip packaging

1. Introduction

In traditional integrated circuit (IC) packaging, the silicon chip is wire-bonded to a lead frame and sealed by a ceramic or plastic shell. Continuous improvement of microprocessor performance involves the increase in electronic packing density, device speed and size reduction. This has created high demands for smaller, cheaper, and lighter assemblies for high volume production. The driving forces for advanced packaging technologies are size reduction and device speed improvement. In advanced packaging and interconnection assemblies, the package size and the number of interconnects in the package are greatly reduced by using surface mount technology. Among the advanced packaging techniques, flip chip packaging is receiving increasing attention [1–4].

Flip chip packaging technology is an interconnect technology which was first invented by IBM over 30 years ago as a packaging solution for high performance computers [5]. In this technology, the active area of the silicon chip surface is mounted facing toward the substrate by a variety of interconnect materials and methods [4]. Compared with traditional face-up wire bonding and tape automated bonding (TAB), the flip chip process provides higher packing density, shorter interconnection length, better electrical performance, improved reliability, and better manufacturability. Over the past 10 years, great efforts have been devoted to the research and development of flip chip technology. One of the most successful flip chip packaging processes is the controlled collapsible chip connection (C4) [1], as shown in Fig. 1.

* Corresponding author.

0040-6031/00/$ – see front matter
PII: S0040-6031(00)00357-9

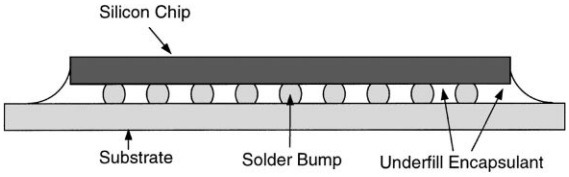

Fig. 1. Illustration of C4 flip chip packaging.

A major challenge for the flip chip packaging technique originates from thermal stresses caused by the mismatch of coefficient of thermal expansion (CTE) between the silicon chip and the organic substrate [6], as demonstrated in Table 1. In particular, this mismatch produces thermal stresses on solder joints which results in fatigue and crack growth during temperature cycles [7]. This is a major reliability concern because cracks increase thermal and electrical resistance which lead to component failure. To solve this problem, a silica filled epoxy resin with low CTE is used to fill the gap between the silicon chip and the substrate (Fig. 1). This epoxy-based material, called underfill encapsulant, has a CTE which closely matches that of the solder alloy. Therefore, this encapsulation provides mechanical reinforcement and reduces thermal stresses on the solder joints. Consequently, the thermal properties of the underfill material have a direct impact on the reliability of the solder joints. For this reason, the development and characterization of epoxy-based packaging materials are of great interest to the microelectronics industry [8].

In this paper, we studied the thermal properties of an epoxy-based underfill encapsulant which was developed for Intel's next generation flip chip (C4) packaging. The cure behavior, weight loss profile, filler size distribution and morphology, thermal expansion and dynamic mechanical properties were investigated using differential scanning calorimetry (DSC), thermogravimetric analysis (TGA), scanning electron microscopy (SEM), thermomechanical analysis (TMA) and dynamic mechanical thermal analysis (DMTA). These experimental results were used to improve the manufacturing process.

Table 1
Material properties of flip chip packaging

Material	Young's Modulus (GPa)	Poisson's ratio	CTE (10^{-6}/°C)
[a]Solder (37% Sn–67% Pb)	6	0.40	24
[b]Encapsulant	8	0.30–0.35	24
[c]Silicon (chip)	131	0.30	2.8
[c]FR-4PCBs, *x* or *y*	22	0.28	18
[c]FR-4PCBs, *z*	22	0.28	70

[a] From [6].
[b] This work.
[c] From [4].

2. Experimental

The C4 underfill encapsulant was developed by Intel and its material supplier. The encapsulant was stored in a −40°C freezer before the experiments. At room temperature, this uncured epoxy-based material is a black viscous liquid. The chemistry of this epoxy will not be discussed here because it contains proprietary information.

2.1. DSC

The curing reaction of the underfill epoxy was examined by a Perkin–Elmer DSC-7 system. Each epoxy sample was sealed in a DSC hermetic pan. Both non-isothermal (scanning) and isothermal DSC modes were used. Non-isothermal DSC experiments were performed at heating rates of 1, 2, 5, 7.5, and 10°C/min from 25 to 300°C. Isothermal DSC experiments were conducted between 100 and 145°C. For isothermal DSC experiments, the samples were placed in the DSC cell at 25°C. The temperature was then increased rapidly to the pre-selected temperature for the isothermal measurement. The heat flow as a function of time was recorded and analyzed. The time needed to reach the isothermal temperature (typically about 2–3 min) was excluded from the analysis. For this particular epoxy, the curing reaction rate prior to reaching the isothermal temperature was negligible.

2.2. TGA

All TGA measurements were conducted in an air atmosphere on a TA Instruments TGA 2950 Thermogravimetric Analyzer, which has a sensitivity of 0.1 μg. The weight loss during cure was analyzed. In addition, the filler content of this epoxy was

measured by TGA upon heating the uncured material from room temperature to 600°C at 5°C/min.

2.3. SEM

Silica filler morphology and size distribution, which strongly affect flow characteristics, were investigated by a Philips XL 40 FEG scanning electron microscope (SEM). Both secondary electron and back scattered electron imaging were used. A thin layer of gold was coated on the sample surface to provide electrical conduction and reduce surface charging.

2.4. TMA

Linear thermal expansion coefficient of cured samples was measured from −60 to 250°C using a Perkin–Elmer TMA-7 thermal mechanical analyzer operated in expansion mode. Cylindrical samples with a typical sample height of approximately 4 mm were cured using following two different thermal profiles:

1. 25–120°C at 3°C/min, isothermal at 120°C for 30 min, 120–150°C at 1.5°C/min, isothermal at 150°C for 165 min;
2. 25–80°C at 5°C/min, isothermal at 80°C for 15 min, 80–87°C at 0.31°C/min, 87–105°C at 0.67°C/min, 105–150°C at 2.37°C/min, isothermal at 150°C for 84 min.

TMA data were obtained at a heating rate of 5°C/min. To minimize viscous flow during the measurements, especially above the glass transition temperature T_g, all TMA measurements were performed with a small loading force of 5 mN.

2.5. DMTA and DMA

Dynamic mechanical properties of cured samples were determined from −50 to 250°C using DMTA and DMA techniques. DMTA experiments were performed on a Rheometric Scientific DMTA 3E operated in rectangular tension mode. During each experiment, the dynamic strain was kept at 0.03%. DMA measurements were carried out on a Perkin–Elmer DMA-7 dynamic mechanical analyzer operated under three point bending mode. The width of the bending platform was 20 mm. During both DMTA and DMA experiments, the static force was kept at 120% of the dynamic force and the frequency of the dynamic force was maintained at 1 Hz.

3. DSC study of curing reaction

It is very important to understand the curing reaction of an epoxy-based underfill material, because its physical and mechanical properties depend on the extent of cure. DSC is one of the most widely used thermal analysis techniques to characterize the epoxy curing reactions [9,10]. Fig. 2 shows non-isothermal DSC scans at various heating rates. Notice that the exothermic reaction peak is very sharp, indicating that this underfill epoxy can be cured rapidly near 150°C. This is highly desirable because the processing time can be significantly reduced. Also notice that the exothermic reaction has at least two overlapped peaks, implying that the cure reaction occurs in two or more stages. The first stage is much sharper when compared with the second stage, especially at heating rates greater than 5°C/min. Based on our DSC scans at heating rates of 1 and 2°C/min, the average enthalpy of the curing reaction was determined to be 144.7±2.8 J/g.

Scanning DSC measurements generally require much less time than isothermal experiments, therefore, they can be used to provide quick results on physical and chemical reactions. However, the construction of a proper baseline in a non-isothermal DSC measurement is almost always a problem, because the

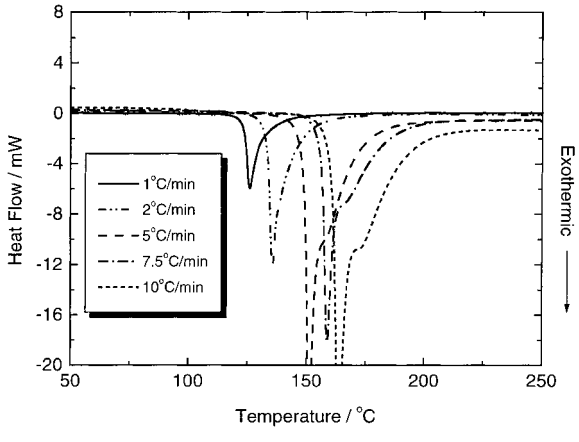

Fig. 2. DSC scans of an epoxy-based underfill material at various heating rates.

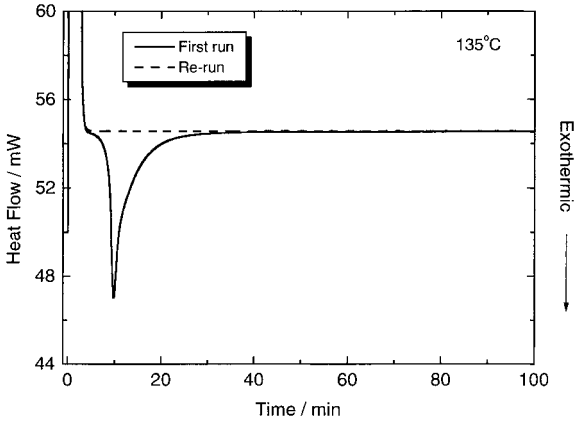

Fig. 3. Isothermal DSC scan at 135°C. In this experiment, the DSC sample was heated from 25 to 100°C at 80°C/min, then heated from 100 to 135°C at 20°C/min. The initial heating ramp was included in this plot.

change in sample heat capacity accompanying a transition can shift the baseline substantially [9,10]. This effect can be seen in Fig. 2, where the DSC baseline shifted significantly during the curing reaction when the DSC heating rate was greater than 5°C/min.

Isothermal DSC was also employed to study the curing reaction. The advantage of isothermal DSC is that during the curing reaction, time and temperature effects are de-coupled, and changes in sample heat capacity will not cause any shift in the DSC baseline, since the heating rate $dT/dt=0$. Fig. 3 is an isothermal DSC curve measured at 135°C. After the first run, the same test was repeated using the same sample. The second run provides a very good baseline for isothermal DSC. Fig. 4 (a) and (b) plot several isothermal DSC curves at various temperatures. From isothermal DSC data, the heat of reaction was determined to be 143.9±2.8 J/g, which agrees with the results of non-isothermal DSC scans. It should be pointed out that below 120°C, the curing reaction stops after approximately 90% conversion fraction. Subsequent non-isothermal DSC scans showed a small exothermic peak near 150°C.

A general equation used in DSC kinetics analysis can be expressed as [9,10]

$$\frac{d\alpha}{dt} = kf(\alpha) \tag{1}$$

where α and $d\alpha/dt$ are the fractional conversion and the conversion rate at time t, respectively, k is the apparent

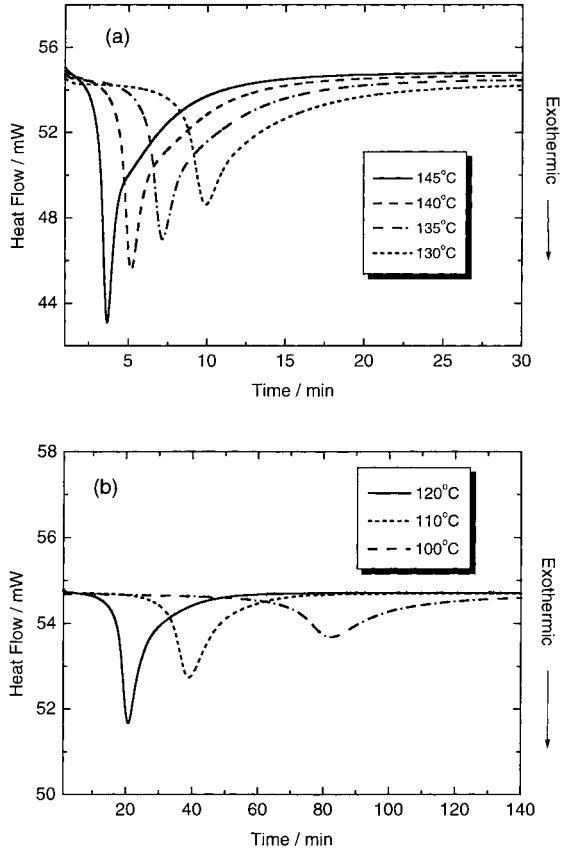

Fig. 4. Isothermal DSC traces at (a) 145°C, 140°C, 135°C and 130°C; (b) 120°C, 110°C and 100°C. The initial heating ramps were excluded from the plots.

rate constant which is assumed to be of Arrhenius form:

$$k = A\exp\left(\frac{-E}{RT}\right) \tag{2}$$

where A is a constant, E is the apparent activation energy, R is the gas constant and T is the absolute temperature. For simple nth-order reactions, $f(\alpha)=(1-\alpha)^n$ and the heat release rate dH/dt, which is proportional to $d\alpha/dt$, will decrease monotonically with time. Isothermal DSC results clearly reveal that nth-order reaction mechanism alone cannot describe the curing of the epoxy-based underfill material, because an exothermic peak is found at non-zero time, as shown in Fig. 4. This can only be due to auto-catalytic and/or consecutive reactions [10].

Based on isothermal DSC results, the conversion fraction as a function of time is plotted in Fig. 5 for

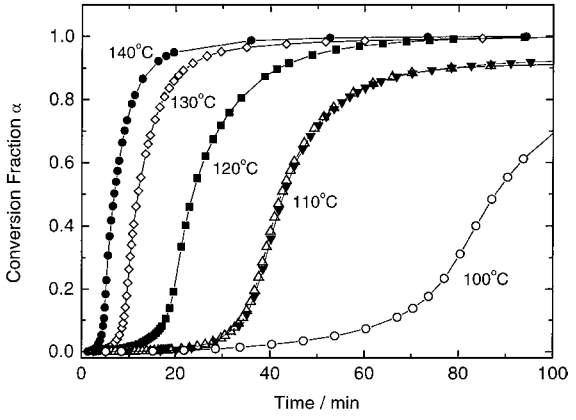

Fig. 5. Conversion fraction α as a function of time at different temperatures.

several isothermal temperatures. Results at 110°C were obtained from two independent isothermal runs, indicating good experimental repeatability. Above 130°C, it takes less than 20 min to achieve 90% conversion fraction (see also Figs. 3 and 4), again demonstrating that this material can be cured rapidly. However, when the curing temperature is below 120°C, it is difficult to obtain a fully cured sample.

Based on isothermal DSC results, we can plot the reaction onset time, t_{onset}, as a function of the inverse temperature, $1/T$, as shown in Fig. 6. From the slope of ln (t_{onset}) against $1/T$ plot, the apparent activation energy for the curing reaction can be deduced, which was determined to be 89.1±0.2 kJ/mol. Based on this activation energy, the onset time of cure at 25°C is estimated to be ~67 days. This is in agreement with the underfill shelf life data provided by supplier. The thermal stability of the underfill epoxy is significantly better at the storage temperature of −40°C.

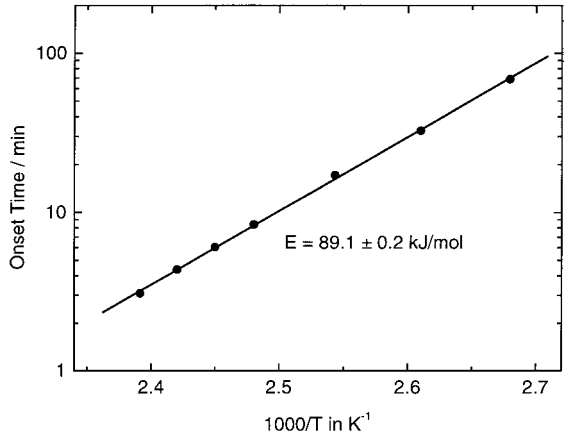

Fig. 6. Onset time for the curing reaction as a function of 1000/T. The slope of ln (t_{onset}) vs. $1/T$ line is E/R. In this figure, the slope of the straight line is $E/(1000R\ln 10)$, from which E is found to be 89.1±0.2 kJ/mol. At t_{onset}, the conversion fraction is approximately 5–8%.

4. Weight loss profile and filler content

Fig. 7(a) shows a TGA curve during a typical curing process. During this process, the temperature of the uncured underfill epoxy was raised from 25 to 120°C at 3°C/min, then kept isothermally at 120°C for

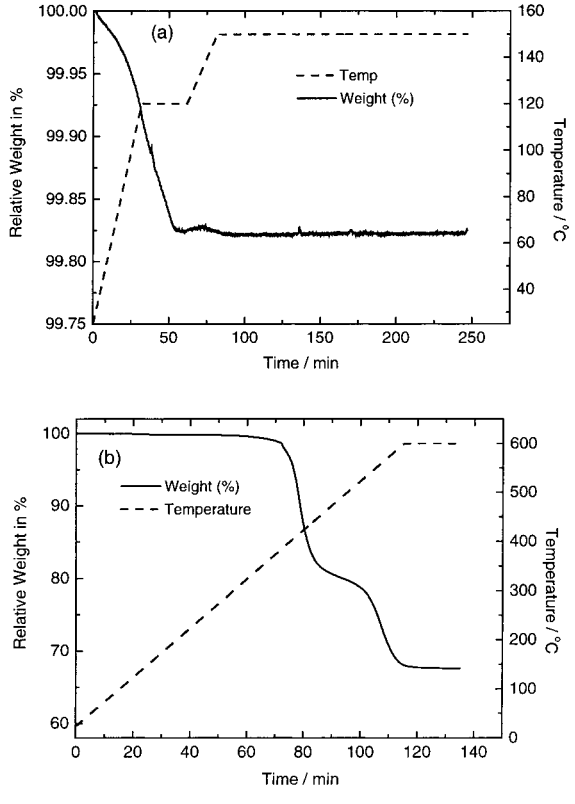

Fig. 7. (a) TGA weight loss curve of the underfill epoxy during a typical curing process. (b) TGA curve of an uncured underfill epoxy sample when heated to 600°C. Notice that below 300°C, the weight loss is minimal.

30 min before being raised to 150°C at 1.3°C/min. The total isothermal time at 150°C was 166 min. From Fig. 7(a), it is clear that the weight loss was completed during the 30 min isothermal at 120°C, and the total weight loss during cure was only 0.18%. The low cure volatile of this epoxy yields almost 100% solid.

To provide mechanical strength and to reduce the CTE of the epoxy resin, silica fillers were added to the underfill epoxy. The filler content of the underfill epoxy can be easily determined by TGA. Fig. 7(b) is a TGA plot, which shows the total weight loss upon heating the uncured epoxy to 600°C. The degradation of the underfill material has two distinct major stages. The onset temperature of the first degradation stage was determined to be 390°C, and the onset temperature of the second degradation was 536°C. The total weight loss is 32.41%, which leads to a total filler content of 67.59%. TGA data showed that this epoxy-based underfill material has a rather high degradation temperature in an air atmosphere, indicating that the thermal stability of this material is excellent.

5. Filler morphology

The morphology and size distribution of these silica fillers were analyzed using SEM. Fig. 8(a) is a low-magnification SEM micrograph showing the filler distribution. From this SEM micrograph, it is clear that all fillers are spherical in shape, and the largest filler particles are approximately 25 μm in diameter with no segregation observed, i.e., small and large fillers are randomly distributed across the sample. This leads to isotropic properties for the material. Fig. 8(b) is a high-magnification SEM micrograph. The smallest fillers are about 0.4 μm in diameter.

6. Thermal expansion behavior

Samples used for TMA studies were prepared using cure profiles labeled as A and B, as discussed before. As suggested by isothermal DSC experimental results, both cure profiles should yield nearly fully cured materials. In practice, it has been shown that cure profile B may reduce void formation in the cured materials. This is because that cure profile B has an additional isothermal step at 80°C, this will initiate a slower reaction rate, which allows cure volatiles to escape instead of being trapped.

Fig. 9 shows the TMA results of cured C4 underfill epoxy samples prepared using profiles A and B. The relative increase in sample length, $\Delta L/L_0=(L-L_0)/L_0$, was measured during continuous heating at 5°C/min and normalized to the initial sample length L_0 at −60°C. For the samples presented in Fig. 9, the thermal expansion behavior are practically identical. When the temperature approaches 125°C, the slope of

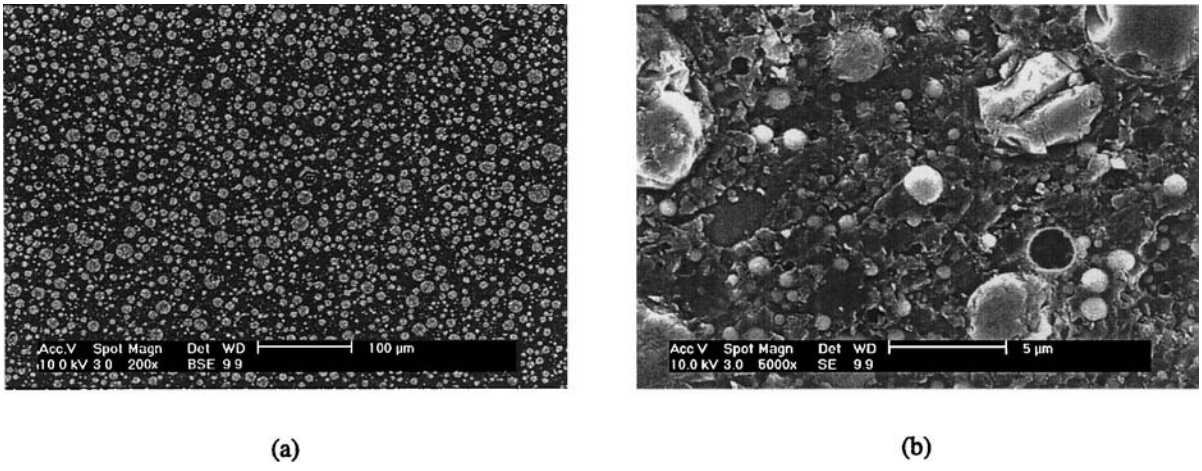

Fig. 8. (a) SEM micrograph showing that all fillers are spherical in shape, and they are randomly distributed without segregation. (b) High-magnification SEM micrograph showing the local morphology of the underfill material.

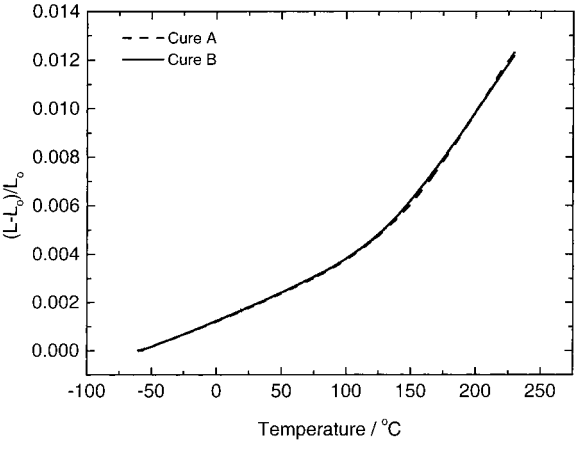

Fig. 9. Relative increase in sample length heated at 5°C/min. L_0 is the length at −60°C. Samples cured using profiles A and B exhibit nearly identical expansion behavior over the entire measured temperature range.

the $\Delta L/L_0$ curve increases rapidly, which is the signature of the glass transition. Close examination also revealed that for $T<T_g$, $\Delta L/L_0$ is not linearly dependent on temperature, indicating that α is not constant but temperature dependent.

The linear thermal expansion coefficient, $\alpha=\mathrm{d}\ln L/\mathrm{d}T$, is plotted as a function of temperature in Fig. 10.

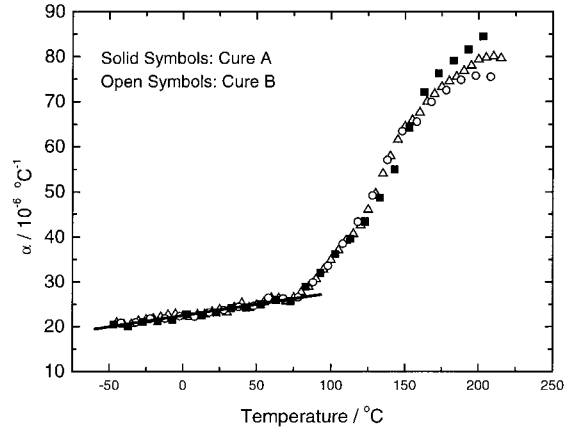

Fig. 10. Linear thermal expansion coefficient α as a function of temperature. Different symbols represent different samples. Solid symbols represent data obtained from samples cured using profile A, whereas open symbols were obtained from samples cured using profile B. Between −60 and 90°C, α increases linearly as a function of temperature and the solid line represents the least square linear fit using Eq. (3).

Below 90°C, α increases gradually with temperature, from 19.4×10^{-6} 1/°C at −60°C to 26.7×10^{-6} 1/°C at 85°C. Between −60 and 90°C, α can be approximated by:

$$\alpha = 22.46\times10^{-6} + 5.04\times10^{-8}T\,(1/^{\circ}\mathrm{C}) \qquad (3)$$

where T is in Celsius. At room temperature, CTE of the cured epoxy is 23.7×10^{-6} 1/°C, which is rather low, and closely matches the CTE of the solder alloy (see Table 1). Therefore, the thermal stresses on solder ball joints can be drastically reduced. When temperature approaches 90°C, α begins to deviate from the above linear behavior, signaling the beginning of the glass transition. When the glass transition temperature T_g is approached, the molecular mobility of the polymer chains increases and the glassy solid becomes a viscous liquid, thus α increases rapidly, as shown in Fig. 10.

7. Dynamic mechanical properties

It is important to understand the dynamic mechanical properties of underfill materials, because they strongly affect thermal stresses and silicon die warpage in the packaging. The dynamic mechanical properties of cured C4 epoxy were measured by DMTA. In addition, dynamic mechanical analysis is more sensitive in detecting T_g [11]. Fig. 11 shows the storage modulus E', loss modulus E'' and the loss

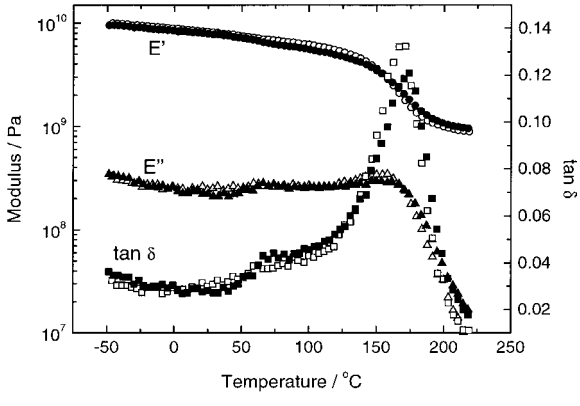

Fig. 11. DMTA scans for underfill epoxy. Solid symbols represents data obtained from samples cured using profile A, and open symbols were obtained using cure profile B.

factor tan δ for underfill epoxy. Again, samples prepared using cure profiles A and B have nearly the same E', E'', and tan δ curves, indicating that both cure profiles generate completely cured samples.

From Fig. 11, it can be determined that the storage modulus at -50°C is approximately 9.5 GPa. As the temperature increases, E' decreases gradually. At 25°C, E' is about 8.2 GPa. When T approaches 125°C, E' decreases rapidly. At the same time, E'' develops a rather broad peak near 156°C and a tan δ peak appears at about 170°C. These two temperatures can both be assigned as the glass transition temperature. These dynamic mechanical properties were also verified by DMA measurements performed using a Perkin–Elmer DMA 7, operated in three-point bending mode [12].

Based on TMA and DMTA data, the stress index $\alpha(T)E(T)$ of this cured underfill epoxy is approximately a constant below T_g: $\alpha(T)E(T) \sim 0.2$ MPa/°C, which is rather low. Finite-element modeling results showed that with the application of underfill epoxy, the maximum normal strain in the outermost solder joint of the package can be reduced by 15%. At the same time, there is virtually no change in the tensile bending stress on the exposed silicon chip [13]. Therefore, the application of underfill epoxy greatly improves solder joint reliability.

8. Conclusions

An epoxy-based underfill encapsulant material developed for Intel's next C4 flip chip packaging has been characterized using thermal analysis techniques. DSC measurements showed that this material can be cured rapidly at the processing temperature of 145°C with no post-cure required. Isothermal DSC results showed that the apparent activation energy for cure is 89.1 kJ/mol, which results in a good thermal stability at room and storage temperatures. TGA weight loss analysis revealed that this material has less than 0.2% weight loss during the curing reaction, and the onset temperature of degradation is as high as 390°C. TGA analysis also showed that the silica filler content is about 67%. SEM micrographs revealed that the fillers are spherical and they are randomly distributed without segregation. TMA analyses on fully cured underfill samples showed that below 90°C, the linear thermal expansion coefficient α increases linearly as a function of temperature. At room temperature, α is about 23.7×10^{-6} 1/°C, which closely matches that of the solder alloy. Above 90°C, α deviates from linear temperature dependence and increases faster as the temperature increases, indicating the beginning of the glass transition. Both DMTA and DMA measurements showed that this material has a room temperature modulus of about 8.2 GPa. The measured CTE and modulus data indicated that this epoxy has a low stress index. The application of this epoxy-based underfill encapsulant greatly improves the solder joint reliability in Intel's C4 flip chip packaging.

Acknowledgements

Y. He wishes to thank Dr. Yuejin Guo for useful discussion and comments on this study.

References

[1] D.R. Halk, Surface Mount Tech. (1997) 54 Sept.
[2] C.A. Harper (Ed.), Electronic Packaging & Interconnection Handbook, 2nd Edition, McGraw-Hill, New York, 1997.
[3] K. Boustedt, E.J. Vardaman, Microelec. Int. 14 (3) (1997) 31.
[4] J.H. Lau (Ed.), Flip Chip Technologies, McGraw-Hill, New York, 1995.
[5] E. Davis, W. Harding, R. Schwartz, J. Corning, IBM J. Res. Devel. (1964) 102 April.
[6] Yutaka Tsukada, Yohko Mashimoto, Toshihiko Nishio, Nobuo Mii, Proc. 1992 Joint ASME/JSME Conf. Electronic Packaging, in: W.T. Chen, Hiroyuki Abe (Eds.), Materials and Processes, Reliability, Quality Control and NDE, American Society of Mechanical Engineers, New York, 1992, pp. 827–835.
[7] S.C. Machuga, S.E. Lindsey, K.D. Moore, A.F. Skipor, Proc. IEEE/CHMT Intl. Electron. Manufact. Technol. Symp., 1992, pp. 53–58.
[8] R. Ghoshal, M. Sambasivam, P.K. Mukerji, Microelec. Int. 14 (3) (1997) 12.
[9] J.M. Barton, Adv. Polym. Sci. 72 (1985) 111.
[10] G.W.H. Höhne, W. Hemminger, H.-J. Flammersheim, Differential Scanning Calorimetry: an Introduction for Practitioners, Springer, New York, 1996.
[11] R.P. Chartoff, P.T. Weissman, A. Sircar, in: R.J. Seyler (Ed.), Assignment of the Glass Transition, ASTM, Philadelphia, 1994.
[12] Y. He, Intel Corporation, unpublished results, 1997.
[13] A. Kirtikar, M. Kuroda, J. Kubota, O. Raiser, R. Mahajan, S. Ramalingam, Intel Internal Report, 1997.